

# Strong Correlation Effects in the Fullerene C<sub>20</sub>

Fei Lin,<sup>1</sup> Erik S. Sørensen,<sup>2</sup> Catherine Kallin,<sup>2</sup> and A. John Berlinsky<sup>2</sup>

<sup>1</sup>*Department of Physics, University of Illinois at Urbana-Champaign, Urbana, Illinois 61801, USA*

<sup>2</sup>*Department of Physics and Astronomy, McMaster University, Hamilton, ON, L8S 4M1 Canada*  
(Dated: May 17, 2021)

The smallest fullerene, dodecahedral C<sub>20</sub>, is studied using a one band Hubbard model parameterized by  $U/t$ . Results are obtained using exact diagonalization of matrices with linear dimensions as large as  $5.7 \times 10^9$ , supplemented by quantum Monte Carlo. We report the magnetic and spectral properties of C<sub>20</sub> as a function of  $U/t$  and investigate electronic pair binding. Solid forms of C<sub>20</sub> are studied using cluster perturbation theory and evidence is found for a metal-insulator transition at  $U \sim 4t$ . We also investigate the relevance of strong correlations to the Jahn-Teller effect in C<sub>20</sub>.

PACS numbers: 71.10.Li, 71.20.Tx, 71.30.+h

The smallest fullerene, C<sub>20</sub>, contains 12 carbon pentagons (and no hexagons) forming a dodecahedron in a perfect representation of a platonic solid. Among the many possible isomers of C<sub>20</sub>, it is not obvious that this dodecahedral fullerene cage should be the most stable and theoretical studies [1, 2] have reached different conclusions. In addition, unlike C<sub>60</sub>, dodecahedral C<sub>20</sub> is not spontaneously formed in condensation or cluster annealing processes [3], and its extreme curvature and strong reactivity led to doubts about its stability. It therefore created considerable excitement when Prinzbach et al. [4] succeeded in producing the dodecahedral fullerene isomer of C<sub>20</sub> in the gas-phase. Experiments have also shown evidence for solid phases of C<sub>20</sub> [5, 6] although the crystal structure is still debated. Density-functional studies of the solid forms of C<sub>20</sub> [6, 7, 8, 9] have suggested different crystal structures with the most promising candidate, C<sub>20</sub> cages connected by C atoms to form a 22 atom unit cell [6, 9], predicted to become superconducting upon doping with Na.[9] A simple-cubic-like phase of C<sub>20</sub> has also been speculated to become superconducting [8]. In their proposal for a purely electronic mechanism for superconductivity in C<sub>60</sub>, Chakravarty, Gelfand and Kivelson [10] have stressed the importance of structure at the mesoscale [11]. Along with the molecular solids formed by C<sub>60</sub>, solid phases of C<sub>20</sub> would be ideal candidates for this picture, and a detailed understanding of these phases would be of great interest. Strong correlation effects are likely to be very important in C<sub>20</sub>, and previous studies [1, 2, 6, 7, 9, 12] have treated these correlation effects approximatively. Here, we show that within a Hubbard model description, an almost exact treatment is possible using a large-scale numerical approach.

Our starting point is the one-band Hubbard Hamiltonian on a single C<sub>20</sub> molecule defined as:

$$H = -t \sum_{\langle ij \rangle \sigma} (c_{i\sigma}^\dagger c_{j\sigma} + h.c.) + U \sum_i n_{i\uparrow} n_{i\downarrow}, \quad (1)$$

where  $c_{i\sigma}^\dagger$  ( $c_{i\sigma}$ ) is an electron creation (annihilation) operator,  $U$  is the on-site Coulomb interaction and  $n_{i\sigma}$  is

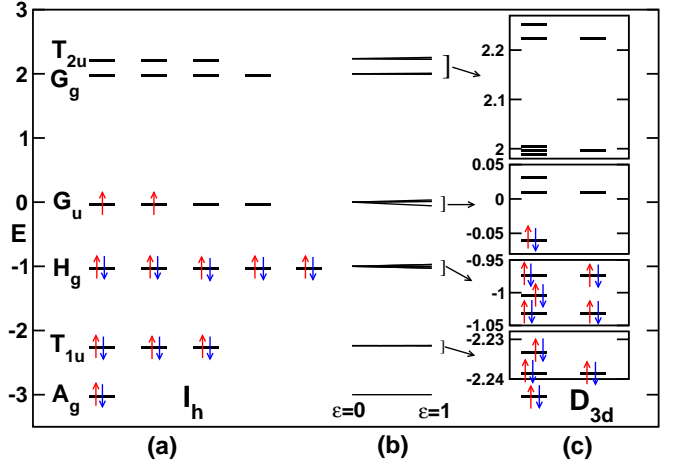


FIG. 1: (Color online). (a) HMO levels for neutral C<sub>20</sub> with  $I_h$  symmetry. (b) The Walsh diagram showing the evolution of the levels with the distortion,  $\epsilon$ , towards  $D_{3d}$  symmetry. (c) HMO levels for the molecule with  $D_{3d}$  symmetry ( $\epsilon = 1$ ).

the number of electrons on site  $i$  with spin  $\sigma$ . Due to the extreme curvature of C<sub>20</sub> we expect  $t$  to be smaller than typical values for C<sub>60</sub> while  $U$  should remain close to that of C<sub>60</sub>. Consequently, we expect that a realistic value for  $U/t$  valid for C<sub>20</sub> is likely *larger* than the value of  $U/t \sim 4$  [31] used for C<sub>60</sub>, implying that strong correlation effects play a more crucial role in the physics of C<sub>20</sub>. Even though C<sub>60</sub> and C<sub>20</sub> share the same symmetry group,  $I_h$ , non-interacting C<sub>20</sub> is a metal while C<sub>60</sub> is an insulator. This is evident from the Hückel molecular orbitals (HMO) shown in Fig. 1a. The highest occupied molecular orbital (HOMO),  $G_u$ , is fourfold degenerate, containing 2 electrons for the neutral molecule. The lowest unoccupied molecular orbital (LUMO),  $G_g$ , is considerably higher in energy. Here we shall mainly be concerned with the neutral, 1- and 2-electron doped molecule which only involves the  $G_u$  levels.

Due to the orbital degeneracy of the neutral C<sub>20</sub> molecule, the Jahn-Teller effect is likely to be important.

	$U = 2t$	$S$ $j$	$U = 5t$	$S$ $j$
$I_h$	-20.5983834340	1 $0, \pm 2$	-12.1112842959	0 5
	-20.5981592741	1 $\pm 4$	-12.0123014488	0 $0, \pm 2, \pm 4$
	-20.5920234655	0 $\pm 2$	-11.8770332831	1 $0, \pm 2$
	-20.0527029539	0 5	-11.8472120431	1 $\pm 1, \pm 3$
$D_{3d}$	-20.6757641960	1 0	-12.1204684092	0 3
	-20.6462557924	1 $\pm 2$	-12.0921677742	0 0
	-20.6166968560	0 $\pm 2$	-11.9197052918	1 3
	-20.0754248172	0 3	-11.8974914914	1 0

TABLE I: Lowest energy levels (in units of  $t$ ) of the neutral  $C_{20}$  molecule for  $U = 2t, 5t$ , labeled by spin and pseudo-angular momentum, for the  $I_h$  ( $j = j_{10}$ ) and  $D_{3d}$  ( $j = j_6$ ) configurations.

The electronic  $G_u$  levels can couple to the  $A_g$ ,  $G_g$  and  $H_g$  Jahn-Teller phonon modes. Theoretical studies have argued for the resulting lowered symmetry to be  $C_2$  [13],  $D_{5d}$  [14],  $C_{2h}$  [15],  $C_i$  [16] and  $D_{3d}$  [2, 17]. Here we follow Yamamoto et al. [17] and assume a static deformation of  $D_{3d}$  symmetry. The bond lengths for the optimal  $D_{3d}$  structure are [17]  $a_{ab} = 1.464\text{\AA}$ ,  $a_{bc} = 1.469\text{\AA}$ ,  $a_{cc'} = 1.519\text{\AA}$ , and  $a_{cc''} = 1.435\text{\AA}$ . (See Fig. 1 of Ref. 17.) We parameterize the distortion by letting  $t_a$ , the hopping along the bond of length  $a$ , depend on a parameter  $\varepsilon$  in the following way:  $t_a/t = 1 - \varepsilon(a - \bar{a})/\bar{a}$ . Here,  $\bar{a} = 1.4712\text{\AA}$  is the average over  $C_{20}$  of the above bond lengths. Then  $\varepsilon = 0$  and  $1$  correspond to the  $I_h$  and  $D_{3d}$  structures, respectively. At  $\varepsilon = 1$  the maximal deviation of  $t_a/t$  from  $1$  is less than  $3.5\%$ . In Fig. 1, the Walsh diagram for the evolution of the  $I_h$  levels with the distortion  $\varepsilon$  is shown along with the HMO levels for the optimal  $D_{3d}$  structure for  $\varepsilon = 1$ .

*Numerics* – Our exact diagonalization (ED) work is performed in a completely parallel fashion using SHARCnet facilities. In addition to total particle number and total  $S_z$  component of the spin, we also exploit the  $S_{10}$  ( $S_6$ ) sub-group symmetry present in the  $I_h$  ( $D_{3d}$ ) symmetry group. The basic element of this sub-group is a rotation of  $2\pi/10$  ( $2\pi/6$ ) around the face of a pentagon (around a vertex) combined with reflection. We denote the corresponding pseudo-angular momenta by  $j_{10}$  ( $j_6$ ). After symmetry reductions, the size of the Hilbert space at half-filling for the singlet states of the neutral molecule is  $3, 418, 725, 024$  for the dodecahedral  $I_h$  configuration and  $5, 699, 353, 088$  for the  $D_{3d}$  distorted configuration. Using  $64$  cpu's, a Lanczos iteration for the  $I_h$  ( $D_{3d}$ ) configuration is completed in  $540$  ( $980$ ) seconds [18]. Dynamical properties are calculated using standard ED techniques [19]. Our quantum Monte Carlo (QMC) work follows standard methods [20] with ground-state energies obtained at  $T = 0$  using projector QMC while spectral functions are obtained from finite temperature,  $\beta = 10/t$ , QMC [20] combined with Maximum Entropy methods [21].

*Magnetic Properties* – From the non-interacting HMO

levels in Fig. 1, it would seem likely that the ground state of the neutral molecule is magnetic at small  $U/t$ . Our ED and QMC work confirms that this is the case for the  $I_h$  configuration for  $U/t \leq 3$ , where the ground state is observed to be an orbitally degenerate triplet,  $S = 1$ , occurring at  $j_{10} = 0, \pm 2$ . Table I gives the few lowest energy levels, labelled by spin and pseudo-angular momentum, for the cases of  $U/t = 2$  and  $5$ . For  $U/t = 5$ , we find that the ground-state for the  $I_h$  configuration is a non-degenerate singlet,  $S = 0$ , occurring at  $j_{10} = 5$ , and separated from the lowest lying excitation, another singlet at  $j_{10} = 0, \pm 2, \pm 4$ , by a gap of  $0.1t$ . The lowest triplet excitation is found at  $j_{10} = 0, \pm 2$ . This ordering of levels continues to hold for larger  $U/t$ , although the energy scale decreases with increasing  $U$ . The degeneracies and excitation gaps at large  $U/t$  agree with ED studies of the dodecahedral  $S = 1/2$  antiferromagnetic Heisenberg model [22]. In fact the ground state energy calculated for neutral  $C_{20}$  in the large  $U$  limit ( $U > 50$ ) can be related to the ED result for the Heisenberg model to the accuracy that the latter has been calculated [23]. From Table I it is clear that the system crosses over from a triplet to singlet ground state between  $U/t = 2$  and  $U/t = 5$ . Assuming an approximately linear dependence on  $U/t$  of the energy of the triplet states at  $j_{10} = 0, \pm 2$  and the singlet at  $j_{10} = 5$ , we estimate that this transition occurs at  $U_c/t \sim 4.10$ , indicated by the solid vertical line in Fig. 2. The fact that the ground-state for the neutral molecule for  $U > U_c$  is a non-degenerate singlet implies that the molecule is *stable* against Jahn-Teller distortions.

Surprisingly, the  $D_{3d}$  distorted molecule follows the same pattern with the exception that at  $U/t = 0$  the unique ground-state is a singlet. However, once  $U/t$  becomes of order of the splitting of the  $G_u$  levels,  $\sim 0.0686$ , the ground-state becomes a triplet. At  $U/t = 0.5$  and  $2$ , we find that this ground-state triplet occurs at  $j_6 = 0$  with a number of low-lying triplet states above it. The Jahn-Teller distortion has therefore completely removed the orbital degeneracy leaving only a Kramer's degeneracy. At  $U/t = 2$ , the lowest-lying excitation is a triplet at  $j_6 = \pm 2$ , and the lowest-lying singlet, with a gap approximately twice as large, is at the same  $j_6 = \pm 2$ . As for the  $I_h$  configuration, we observe that the ground-state is a singlet at  $U/t = 5$  occurring at  $j_6 = 3$ . An analysis similar to the  $I_h$  case yields  $U_c/t \sim 4.19$ , indicated by the crossed vertical line in Fig. 2, very close to the estimate for the  $I_h$  configuration. Again, the system remains in a singlet state for larger values of  $U/t$ .

*Pair Binding* – The purely electronic mechanism for superconductivity [10, 11] is based on a favorable pair binding energy. The pair binding energy is defined as the energy difference between having two extra electrons on the same and on separate molecules:

$$\Delta_b(N+1) = E(N+2) - 2E(N+1) + E(N). \quad (2)$$

When negative, it is favorable to have the two electrons

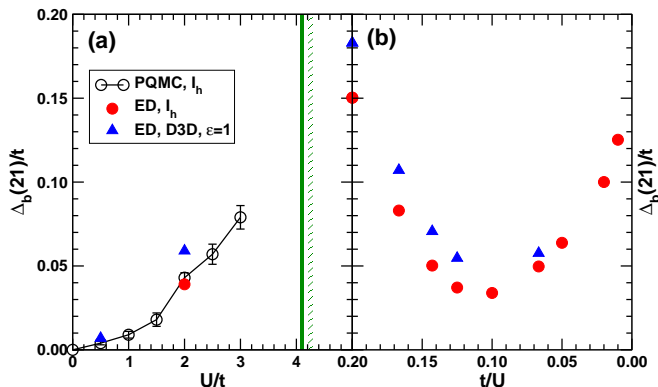


FIG. 2: (Color online). Electronic pair binding energy  $\Delta_b(21)/t$  as a function of  $U/t$ . ED ( $\bullet$ ) and QMC ( $\circ$ ) results for the molecule with  $I_h$  symmetry. ED results ( $\blacktriangle$ ) for the molecule with  $D_{3d}$  ( $\varepsilon = 1$ ) symmetry. The solid (crossed) vertical line indicates  $U_c/t$  for neutral  $I_h$  ( $D_{3d}$ ) molecules. (a)  $\Delta_b$  versus  $U/t$  for  $U/t \leq 5$ . (b)  $\Delta_b$  versus  $t/U$  for  $5 \leq U/t \leq 100$ .

on the same molecule providing a purely electronic mechanism for superconductivity. Intriguingly, for neutral  $C_{12}$  [24], as well as for several related models [11], it is known that  $\Delta_b$  is negative. For  $C_{60}$ , perturbative results indicated that the observed superconducting phase has its origins in a negative  $\Delta_b$  [10, 25, 26]. However, our earlier QMC results [27] find no binding, suggesting that either low order perturbation theory is inadequate or that the QMC results are not sufficiently accurate to measure the binding. Thus it is of considerable interest to obtain exact results for  $C_{20}$  which can then be used to test the accuracy of QMC.

Our results for  $\Delta_b(21)/t$  are shown in Fig. 2. We first consider results for the  $I_h$  configuration of  $C_{20}$ . The QMC results ( $\circ$ ) and the ED results ( $\bullet$ ) are in excellent agreement, and for  $U/t \leq 3$  they show that  $\Delta_b$  is positive and pair binding is *suppressed*. (For  $U > U_c$  it is not possible to perform QMC calculations due to the sign problem.) The ground-state for the neutral molecule is now a singlet and our ED results again clearly indicate that pair binding is *not* favored. As  $U/t$  increases,  $\Delta_b$  reaches a minimum at  $U/t \sim 10$ . Then, as  $U/t \rightarrow \infty$ ,  $\Delta_b$  approaches a finite positive value, consistent with the exact result showing the absence of pair binding for electron doping in the  $U = \infty$  limit [28]. The perturbative results indicating a negative pair binding for  $C_{60}$  were correlated with a violation of Hund's rule for two electron doping [10]. For  $C_{20}$  the same violation of Hund's rule occurs at large  $U$ . For  $U/t \leq 3$ , the ground state with 22 electrons obeys Hund's rule and has  $S = 2$ . However, at  $U/t = 5$ ,  $C_{20}^{2-}$  has an intermediate spin of  $S = 1$  and at  $U/t = 6$  this state has  $S = 0$ , fully violating Hund's rule.

We can only calculate the pair binding for the Jahn-Teller distorted molecule in an approximate manner since

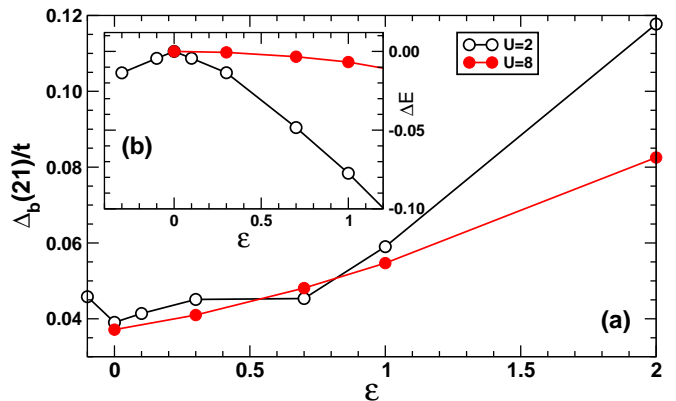


FIG. 3: (Color online). (a) Electronic pair binding energy  $\Delta_b(21)/t$  versus the distortion,  $\varepsilon$ , towards  $D_{3d}$  symmetry, for for  $U/t = 2$  ( $\circ$ ),  $8$  ( $\bullet$ ). The inset, (b), shows the shift in the ground state energy of the neutral molecule,  $\Delta E$ , versus  $\varepsilon$ .

the distortion will depend on the electron doping. We make the simplifying assumption that the distortion is static, of  $D_{3d}$  symmetry, and independent of doping. Since we focus on 1 and 2 electron doping, which only involves  $G_u$  orbitals, it is reasonable to assume that the symmetry of the distortion is the same. Saito et al. [16] find the same symmetry for the neutral and negatively charged molecule. However, the optimal  $\varepsilon$  will show a dependence on the doping which we ignore. Our results for  $\Delta_b$  for the  $D_{3d}$  structure ( $\varepsilon = 1$ ) are shown in Fig. 2 ( $\blacktriangle$ ). For all values of  $U/t$ , we find that  $\Delta_b$  for the  $D_{3d}$  structure is *higher* than for  $I_h$ . The Jahn-Teller distortion appears to work against pair binding. This is confirmed in Fig. 3a, where the pair binding energy is shown as a function of  $\varepsilon$ . In Fig. 3b, we show results for the shift in the ground-state energy versus  $\varepsilon$  where the strong dependence on  $\varepsilon$  for  $U/t = 2$  is indicative of the molecule being Jahn-Teller active. By contrast, for  $U/t = 8$  the dependence on  $\varepsilon$  is very shallow, signalling that the  $I_h$  structure is stable.

*Spectral Functions, Solid  $C_{20}$*  – Next we calculate the density of states,  $N(\omega)$ , and wave-vector dependent spectral functions,  $A(k, \omega) = -(1/\pi)\text{Im}[G(k, \omega + E_0 + i\eta)]$ , for a three-dimensional solid of  $C_{20}$  molecules. Here,  $E_0$  is the ground-state energy and  $G$  the single-particle Green's function. The calculation is performed by cluster perturbation theory (CPT) [29, 30] using QMC and ED data. In all cases, delta-functions were treated as Lorentzians with a broadening of  $\eta = 0.1$ . The QMC version of this method was applied earlier to the case of  $C_{60}$  monolayers [31]. We idealize the hypothetical fcc  $C_{22}$  structure [6, 9], by a model in which the bridging C atoms are replaced by effective hopping integrals,  $t' = -t$ , between  $C_{20}$  molecules. The resulting  $N(\omega)$  and  $A(k, \omega)$ , are shown in Figs. 4 and 5 for  $U/t = 2$  and 5. Also shown in Fig. 4 are the single-molecule densities of states. For  $U/t = 2$ , which lies in the middle of the re-

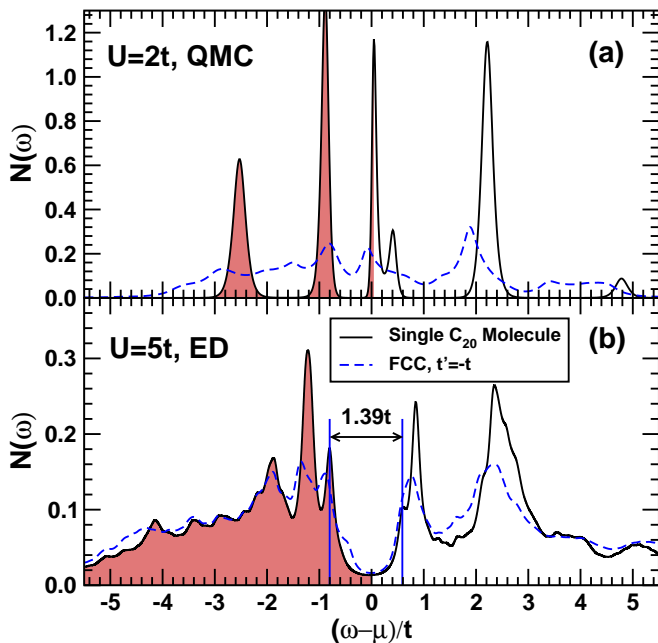


FIG. 4: (Color online). Density of states,  $N(\omega)$ , at  $U = 2t$  (a) from QMC and at  $U = 5t$  (b) from ED. In both panels the DOS for the  $C_{22}$  fcc lattice obtained from CPT with  $t' = -t$  is shown as a dashed line.

gion of triplet ground state, the solid of undistorted  $I_h$  molecules is metallic with a complicated Fermi surface, while, for  $U/t = 5$ , in the region of singlet ground state, the solid is insulating with a gap of about  $1.4t$ .

In conclusion, we have calculated the ground state properties and spectral functions of the Hubbard model on a  $C_{20}$  molecule using ED and QMC. We have identified a ground state crossing at  $U_c \sim 4.1t$  where the system switches from a triplet state which is unstable against a Jahn-Teller distortion to a gapped singlet state which is stable. Extending this result using CPT, we identify a metal-insulator transition for the bulk solid at  $U = U_c$ . If the symmetric,  $I_h$ , form of  $C_{20}$  is found to be stable, a possible explanation would be that it is stabilized by correlations resulting from  $U > U_c$ . Additional results will be presented elsewhere [18].

This project was supported by the NSERC, CIAR and CFI. FL is supported by the US Department of Energy under award number DE-FG52-06NA26170. AJB and CK gratefully acknowledge the hospitality and support of the Stanford Institute for Theoretical Physics, where part of this work was carried out. All the calculations were carried out at SHARCNET supercomputing facilities.

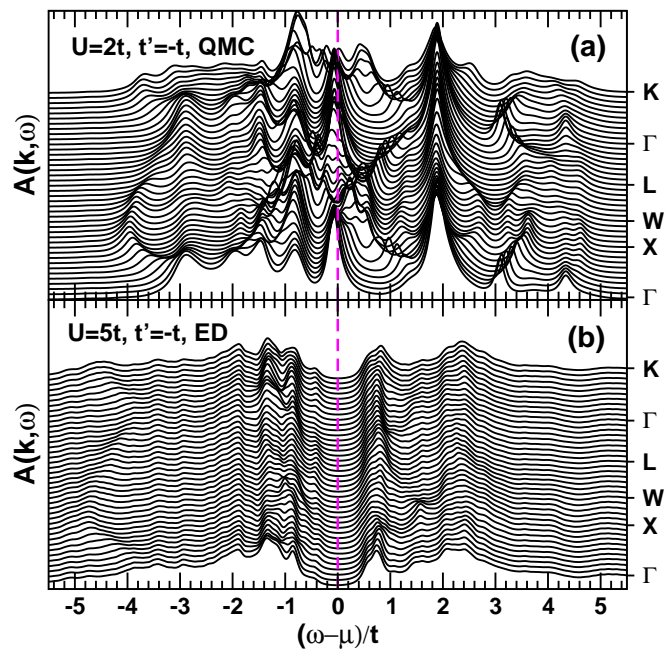


FIG. 5: (Color online). Spectral functions with the chemical potential  $\mu$  determined from  $N(\omega)$  in Fig. 4. Results for the  $C_{22}$  FCC lattice with  $U = 2t$  (a) and  $U = 5t$  (b) as obtained from CPT with  $t' = -t$ . The k-axis labels refer to standard notation for the FCC Brillouin zone.

[1] M. Sawtarie, M. Menon and K. R. Subbaswamy, Phys. Rev. B **49**, 7739 (1994); J. C. Grossman, L. Mitás and

K. Raghavachari, Phys. Rev. Lett. **75**, 3870 (1995); P. R. Taylor, E. Balyska J. H. Weare and R. Kawai, Chem. Phys. Lett. **235**, 558 (1995); R. O. Jones and G. Seifert, Phys. Rev. Lett. **79**, 443 (1997).  
 [2] G. Galli, F. Gygi and J. C. Golaz, Phys. Rev. B **57**, 1860 (1998).  
 [3] H. W. Kroto, Nature **329**, 529 (1987).  
 [4] H. Prinzbach *et al.*, Nature **407**, 60 (2000).  
 [5] Z. Wang *et al.*, Phys. Lett. A **280**, 351 (2001).  
 [6] Z. Iqbal *et al.*, Eur. Phys. J. B **31**, 509 (2003).  
 [7] M. Côté, J. C. Grossman, M. L. Cohen and S. G. Louie, Phys. Rev. B **58**, 664 (1998); S. Okada, Y. Miyamoto and M. Saito, *ibid* **64**, 245405 (2001).  
 [8] Y. Miyamoto and M. Saito, Phys. Rev. B **63**, 161401(R) (2001).  
 [9] I. Spagnolatti, M. Bernasconi and G. Benedek, Europhys. Lett. **59**, 572 (2002).  
 [10] S. Chakravarty, M. P. Gelfand and S. Kivelson, Science **254**, 970 (1991).  
 [11] S. Chakravarty and S. A. Kivelson, Phys. Rev. B **64**, 064511 (2001).  
 [12] R. López-Sandoval and G. M. Pastor, Euro. Phys. J. D **38**, 507 (2006).  
 [13] B. L. Zhang *et al.*, J. Chem. Phys. **97**, 5007 (1992).  
 [14] V. Parasuk and J. Almlöf, Chem. Phys. Lett. **184**, 187 (1991).  
 [15] M. Saito and Y. Miyamoto, Phys. Rev. Lett. **87**, 035503 (2001).  
 [16] M. Saito and Y. Miyamoto, Phys. Rev. B **65**, 165434 (2002).  
 [17] T. Yamamoto, K. Watanabe and S. Watanabe, Phys. Rev. Lett. **95**, 065501 (2005).

- [18] F. Lin, E. S. Sørensen, C. Kallin and A. J. Berlinsky, in preparation (2007).
- [19] E. R. Gagliano and C. A. Balseiro, Phys. Rev. Lett. **59**, 2999 (1987).
- [20] S. R. White *et al.*, Phys. Rev. B **40**, 506 (1989).
- [21] M. Jarrell and J. E. Gubernatis, Phys. Rep. 269, 133 (1996).
- [22] N. P. Konstantinidis, Phys. Rev. B **72**, 064453 (2005).
- [23] For large  $U/t$ , the neutral molecule ground state energy can be fit to  $E_{20}/(t^2/U) = a + b(t/U)^2$ , where  $a = 4E_H/J - 30$  and  $E_H$  is the ground state energy of the Heisenberg model, obtained by exact diagonalization in Ref. 22,  $E_H = -9.72219J$ . A fit, using ED results for  $U/t = 50$  and 100, gives  $E_H = -9.72217J$ .
- [24] S. R. White, S. Chakravarty, M. P. Gelfand and S. A. Kivelson, Phys. Rev. B **45**, 5062 (1992).
- [25] S. Chakravarty and S. Kivelson, Europhys. Lett. **16**, 751 (1991).
- [26] M. Granath and S. Östlund, Phys. Rev. B **66**, 180501(R) (2002).
- [27] F. Lin, J. Šmakov, E. S. Sørensen, C. Kallin and A. J. Berlinsky, Phys. Rev. B **71**, 165436 (2005).
- [28] S. Chakravarty and L. Chayes and S. Kivelson, Lett. Mat. Phys. **23**, 265 (1991).
- [29] D. Sénéchal, D. Perez and M. Pioro-Ladrière, Phys. Rev. Lett. **84**, 522 (2000).
- [30] D. Sénéchal, D. Perez and D. Plouffe, Phys. Rev. B **66**, 075129 (2002).
- [31] F. Lin, E. S. Sørensen, C. Kallin and A. J. Berlinsky, cond-mat/0610823 [Phys. Rev. B (to be published)].